http://www.kidney-international.org

Microarray analysis of a reversible model and an irreversible model of anti-Thy-1 nephritis

M Tsuji[1], T Monkawa[1], J Yoshino[1], M Asai[1], S Fukuda[1], H Kawachi[2], F Shimizu[2], M Hayashi[1] and T Saruta[1]

[1]*Department of Internal Medicine, Keio University School of Medicine, Tokyo, Japan and* [2]*Department of Cell Biology, Institute of Nephrology, Niigata University Graduate School of Medical and Dental Sciences, Niigata, Japan*

A single intravenous injection of anti-Thy-1 monoclonal antibody (mAb) 1-22-3 is known to cause reversible mesangial proliferative glomerulonephritis. However, mAb 1-22-3 injection followed by unilateral nephrectomy leads to progressive glomerulosclerosis and tubulointerstitial change with an irreversible course. To identify genes that play an important role in the irreversible progression of renal injury, we used microarray technology to identify differences in gene expression between these models. Rats were intravenously injected with mAb 1-22-3 1 week after unilateral nephrectomy (irreversible model) or a sham operation (reversible model), and rats were killed on days 4, 7, 14, 42, and 56 after the injection. complementary DNA probes prepared from kidney messenger RNAs were hybridized with oligonucleotide microarrays containing 4854 rat genes. The microarray identified 189 differentially expressed genes, having at least a two-fold difference in expression level between the two models, and they were classified into five clusters. One of the clusters consisted of genes whose expression was markedly upregulated in the irreversible model. This cluster included the genes encoding osteopontin, kidney injury molecule-1, and thymosin β10. Increased expression of thymosin β10 was localized mainly in macrophages in the fibrotic interstitium, and upregulation of thymosin β10 expression was also observed in a unilateral ureteral obstruction model. The microarray analysis yielded information on the molecular mechanisms responsible for the difference in disease progression between the reversible and irreversible model of anti-Thy-1 nephritis. Thymosin β10 may play an important role in the progression of kidney disease.

Kidney International (2006) **69,** 996–1004. doi:10.1038/sj.ki.5000191; published online 25 January 2006

KEYWORDS: anti-Thy-1 nephritis; microarray; thymosin β10

Correspondence: *T Monkawa, Department of Internal Medicine, Keio University School of Medicine, 35 Shinanomachi, Shinjuku-ku, Tokyo 160-8582, Japan. E-mail: monkawa@sc.itc.keio.ac.jp*

Received 14 June 2005; revised 14 October 2005; accepted 31 October 2005; published online 25 January 2006

The common pathological feature of the progressive renal diseases is glomerulosclerosis and tubulointerstitial fibrosis, but the pathogenic mechanisms underlying the progressive renal lesions are poorly understood. Our limited understanding may be attributable to a lack of appropriate animal models, and a model of progressive sclerotic lesions induced by anti-Thy-1 monoclonal antibody (mAb) 1-22-3 in rats has been developed to study the mechanisms of renal disease progression. Anti-Thy-1 nephritis is most commonly used as a model of mesangial proliferative glomerulonephritis; it is self-limiting, and the glomerular architecture returns to normal within 6–8 weeks.[1] A single injection of mAb 1-22-3 to unilaterally nephrectomized rats, on the other hand, causes irreversible glomerulosclerosis and tubular interstitial change (irreversible model), whereas the disease course of the sham-operated rats injected with mAb 1-22-3 is reversible (reversible model).[2–4] In the irreversible anti-Thy-1 nephritis model, urinary protein persists and typical sclerotic renal lesions are observed after a month. Several mechanisms have been proposed to explain the irreversible models, but the actual mechanism of the irreversible model has never been fully elucidated.

In recent years, great advances have been made in techniques to analyze and compare differentially expressed genes, and complementary DNA (cDNA)/oligonucleotide microarray technology is a particularly useful development because it provides parallel and quantitative expression profiles of thousands of genes that can identify genes in a biologic pathway, characterize the function of novel genes, and identify drug targets.

The purpose of this study was to utilize oligonucleotide microarrays to define differences in global changes in renal gene expression between irreversible and reversible models of anti-Thy-1 nephritis, and, specifically, to identify genes that play an important role in disease progression. In the present study, we identified a gene cluster that is upregulated in the irreversible model. Increased expression of thymosin β10 in the cluster was observed mainly in the macrophages in the fibrotic interstitium of the kidney. These findings suggest that osteopontin and thymosin β10 may be involved in the progression of renal disease.

RESULTS

Reversible and irreversible models of anti-Thy-1 nephritis

To produce the reversible anti-Thy-1 nephritis model, rats were sham-operated, and 1 week later injected with mAb 1-22-3. For the irreversible anti-Thy-1 nephritis model, rats were unilaterally nephrectomized, and 1 week later injected with mAb 1-22-3. The time course of urinary protein excretion is shown in Figure 1. Urinary protein excretion peaked at day 7 in both models. The proteinuria in the irreversible model persisted until 2 months after the mAb injection, whereas in the reversible model urinary protein excretion became normal by day 21. No significant urinary protein excretion was seen in the control group of rats unilaterally nephrectomized and not injected with mAb 1-22-3.

Histological analysis of the kidneys on day 4 showed diffuse mesangiolytic changes in both the reversible and irreversible models. On day 14, there were significant increases in glomerular cell number and marked expansion of the mesangial area in both models. By day 56, the mesangial cell proliferation had markedly decreased. Glomerular crescentic lesions and tubulointerstitial changes, including tubular hyaline casts, tubule dilation, and leukocyte infiltration, were more common in the irreversible model. These histological findings are consistent with previous observations.[5]

Gene expression profiles

To identify genes that play an important role in the irreversible progression of renal diseases, we investigated difference in gene expression between the reversible model and irreversible model of anti-Thy-1 nephritis using an oligonucleotide microarray technology. Messenger RNA (mRNA) was prepared from the kidneys of both models at each time point and labeled with Cy-dye during reverse transcription. Labeled cDNAs were hybridized with the microarray slide containing 4854 rat genes, and the expression level of 189 genes differed by more than two-fold between the reversible model and irreversible model at one or more time points. The numbers of differentially regulated genes are shown in Table 1. The majority of the differentially expressed genes were genes that were upregulated at day 4 in the reversible model (167 out of 189 genes, 88.4%). To clarify the function of the 189 differentially expressed genes, they were subjected to clustering analysis based on expression patterns and classified into five clusters (cluster A–E), as shown in Figure 2. The genes identified are tabulated in Table 2.

Cluster A consisted of 13 genes that were differentially expressed in the irreversible model, especially at days 4, 42, and 56. As the microarray results represent the ratio between the mRNA expression in the two models, and do not represent the actual levels of mRNA expression, the mRNA expression levels were examined by semiquantitative reverse transcription-polymerase chain reaction (RT-PCR) for selected genes in cluster A (Figure 3). Semiquantitative PCR analysis revealed that the expression levels of the genes examined peaked at days 7–14, and that the upregulation was more pronounced in the irreversible model than in the reversible model. Thus, the gene expression pattern in this cluster was characterized by upregulation in the irreversible model. The genes whose expression in the kidney differed between the reversible model and the irreversible model of anti-Thy-1 nephritis at days 42 and 56 are shown in Tables 3 and 4, respectively. Most of the cluster A genes were seen in the list of the gene differentially expressed in the progressive phase of the disease.

Cluster C was the largest cluster and contained 170 genes that were differentially expressed in the reversible model at day 4 but for which no clear difference in expression levels was observed between the two models subsequently. Semiquantitative RT-PCR for Aldo-keto reductase family 1 member B7, uridine diphosphate glycosyltransferase 1 family polypeptide A6, and glutathione peroxidase 3 revealed the most striking change in mRNA expression to be a decrease in the irreversible model at day 4 (Figure 3). The functions of the genes in cluster C are in metabolism (83 genes), transport (25 genes), signal transduction (12 genes), developmental

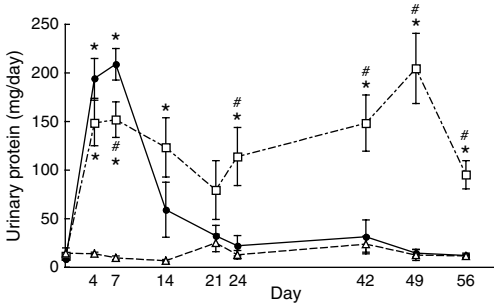

Figure 1 | Time course of urinary protein excretion after mAb 1-22-3 injection. The amount of protein in 24 h urine was measured before the mAb 1-22-3 injection and 4, 7, 14, 21, 24, 42, 49, and 56 days after the mAb 1-22-3 injection. □, irreversible model, unilaterally nephrectomized and injected with mAb 1-22-3; ●, reversible model, sham-operated and injected with mAb 1-22-3; △, control rats, unilaterally nephrectomized and not injected with mAb 1-22-3. Proteinuria persisted for 2 months in the irreversible model, whereas urinary protein excretion in the reversible model became normal by day 21 after the mAb 1-22-3 injection. No proteinuria was detected in control rats. $^{*}P<0.05$ vs control rat. $^{\#}P<0.05$ vs the reversible model.

Table 1 | Numbers of differentially regulated genes revealed by the microarray analysis

	Day after injection				
	4	7	14	42	56
Irreversible > reversible model	13	1	1	8	3
Irreversible < reversible model	167	10	7	2	1

The numbers of genes in the kidney at each time point that were differentially expressed by at least two-fold in the irreversible model (upper row) and in the reversible model (lower row) of anti-Thy-1 nephritis are shown.

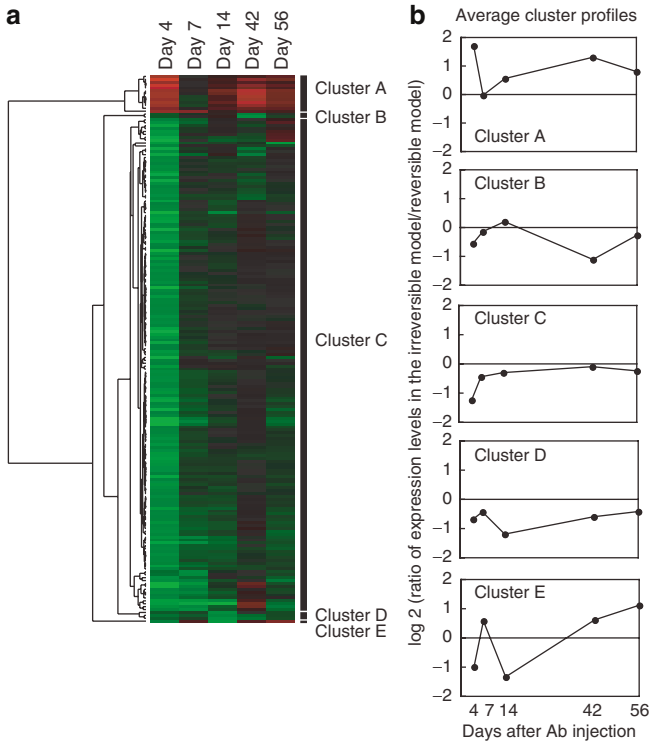

Figure 2 | Cluster analysis of differentially expressed genes identified by microarray analysis of reversible and irreversible models of anti-Thy-1 nephritis. (**a**) Hierarchical clustering of genes whose expression levels differed between the reversible and irreversible models. The temporal expression profiles of 189 genes whose intensity differed two-fold or more between the two models at least at one time point were subjected to hierarchical clustering analysis with CLUSTER software and visualized in a clustergram with TREEVIEW software. Days after antibody injection are represented by columns, and the genes are listed in rows. Green indicates differential expression in the reversible model and red indicates differential expression in the irreversible model at distinct time points. The degree of color saturation reflects the magnitude of the ratio. Black indicates genes whose expression did not differ between the two models. (**b**) Temporal patterns of gene expression within each cluster. The *x*-axis shows the time course and the *y*-axis shows the average value of the log 2 ratios of expression levels in the irreversible model/reversible model.

processes (11 genes), unknown (10 genes), and other (29 genes).

To exclude the possibility that nephrectomy itself affects gene expression, gene expression in unilaterally nephrectomized rats without mAb injection and control rats was compared by microarray analysis; however, no genes were differentially expressed (data not shown).

KIM-1, osteopontin, and thymosin β10

To investigate genes involved in progression of the disease, we focused on analysis of the genes in cluster A, and selected kidney injury molecule-1 (KIM-1), osteopontin, and thymosin β10 for further investigation. Real-time PCR analysis showed that the expression level of all three genes was low in the normal kidney but increased and peaked at day 14, and that their upregulation was more pronounced in the irreversible model than in the reversible model (Figure 4). Overexpression of all the three genes in the irreversible model persisted until days 42 and 56, when the expression in the reversible model decreased.

Cluster A genes in the UUO model

The next step was to determine whether the genes upregulated in the irreversible model were upregulated in another kidney disease model, and we selected the unilateral ureteral obstruction (UUO) model, a well-characterized model of tubulointerstitial fibrosis. Establishment of obstructive nephritis was confirmed by histology and collagen I expression (data not shown). Real-time PCR analysis showed that KIM-1 mRNA was strongly upregulated on the obstructed side in comparison with the control kidney (Figure 5). The increase in expression on the obstructed side peaked at day 4, and gradually decreased thereafter. Osteopontin and thymosin β10 were also upregulated on the obstructed side, but the upregulation persisted until day 21. These findings suggest that KIM-1 expression is more closely associated with the initial kidney insult and that osteopontin and thymosin β10 expression is more related to the progression of kidney disease.

Immunolocalization of thymosin β10

Thymosin β10 expression in renal sections from control rats was low, and very few cells were positive in the tubulointerstitium (data not shown). Thymosin β10 expression was increased in both anti-Thy-1 nephritis models, and its maximal level occurred in the irreversible model at days 7 and 14. Thymosin β10 expression was mainly found in the interstitium (Figure 6a). The immunostaining of Thymosin β10 in the reversible model was weaker than that in the irreversible model at day 14 (Figure 6b). Thymosin β10 expression was also observed in the dilated fibrotic interstitium of the kidney on the obstructed side in the UUO model (Figure 6c). Double immunostaining with anti-thymosin β10 antibody and the macrophage marker ED-1 revealed that most of the cells that were positive for thymosin β10 were macrophages (Figure 6d–f).

DISCUSSION

This study used microarray technology to investigate global gene expression in a model of progressive renal disease in order to elucidate the molecular mechanism of progression of kidney diseases. We used the irreversible anti-Thy-1 nephritis model as the model of progressive renal disease and produced it by intravenously injecting unilaterally nephrectomized rats with mAb 1-22-3. The irreversible anti-Thy-1 nephritis model offers several advantages over other models of chronic renal disease. First, it is easy to produce and yields more reproducible results than the 5/6-nephrectomized rat model, another model of progressive renal disease. Second, it is easy to compare gene expression with the corresponding reversible model because they have the same genetic background. Third, it pursues a progressive course following immune-

Table 2 | Genes whose expression in the kidney differed between the reversible model and the irreversible model of anti-Thy-1 nephritis

Gene accession	Name	Log ratio of differential expression				
		Day 4	Day 7	Day 14	Day 42	Day 56
Cluster A						
AF035963	Kidney injury molecule 1	2.55±0.29	0.09±0.21	0.5±0.49	1.34±0.21	0.95±0.36
U56822	Killer cell lectin-like receptor subfamily A, member 22	2.41±0.10	−0.10±0.16	0.58±0.39	1.25±0.26	0.77±0.36
U87224	Contactin associated protein 1	2.12±0.19	−0.04±0.17	0.44±0.23	0.95±0.31	0.54±0.04
M12199	Collagen, type I, alpha 1	1.68±0.28	−0.15±0.59	0.23±0.81	0.49±0.24	0.73±0.28
AF091577	Olfactory receptor gene Olr1370	1.67±0.27	−0.31±0.10	0.79±0.26	2.02±0.18	1.05±0.19
AF198087	Adrenal secretory serine protease precursor	1.62±0.12	−0.02±0.61	0.87±0.48	1.93±0.04	0.97±0.22
NM_012868	Natriuretic peptide receptor 3	1.62±0.31	−0.35±0.34	0.56±0.53	1.80±0.13	0.95±0.27
NM_012881	Osteopontin	1.54±0.63	0.13±0.37	1.01±0.58	1.98±0.23	1.03±0.07
X89698	Olfactory receptor gene Olr737	1.52±0.59	−0.37±0.23	0.49±0.33	1.41±0.59	0.87±0.15
AF016178	Putative pheromone receptor (Go-VN1)	1.47±0.30	−0.36±0.31	0.55±0.43	1.61±0.05	0.92±0.21
X94551	Laminin, gamma 1	1.46±0.13	−0.09±0.19	0.42±0.27	0.67±0.37	0.44±0.17
AF218574	Meiotic recombination 11 homolog A (S. cerevisiae)	1.43±0.74	1.23±0.74	0.20±0.43	0.68±0.45	0.48±0.33
M58404	Thymosin, beta 10	1.16±0.50	0.02±0.20	0.65±0.18	0.82±0.19	0.76±0.22
Cluster B						
NM_017260	Arachidonate 5-lipoxygenase activating protein	−0.56±0.74	−0.22±1.00	0.17±0.29	−1.01±0.17	−0.20±0.57
M33936	Cytochrome P450, family 4, subfamily a, polypeptide 14	−0.54±0.71	−0.07±0.99	0.24±0.26	−1.21±0.11	−0.34±0.45
Cluster C						
AF182168	Aldo-keto reductase family 1, member B7	−2.38±0.98	−0.10±0.29	−0.48±0.36	0.15±0.47	−0.66±0.64
S70366	UDP glycosyltransferase 1 family, polypeptide A6	−2.33±0.48	−1.08±0.31	−0.44±0.27	−0.01±0.34	−0.80±0.83
D00680	Glutathione peroxidase 3	−2.32±0.13	−0.14±0.44	−0.63±0.05	−0.48±0.14	0.75±0.04
NM_017217	Solute carrier family 7, member 3	−1.96±0.39	−1.31±0.22	−0.26±0.26	0.84±0.22	−0.46±0.56
M83144	Beta-galactoside-alpha 2,6-sialyltransferase	−1.96±0.42	−0.36±0.27	−1.12±0.58	−0.16±0.32	−0.56±0.83
NM_013184	Neurotrophin 5	−1.95±0.25	−0.89±0.16	−0.39±0.27	0.07±0.34	−0.73±0.82
S79716	Class VI alcohol dehydrogenase	−1.93±0.35	−0.84±0.27	−0.34±0.13	−0.01±0.33	−0.70±0.92
NM_012674	Serine protease inhibitor, Kazal type 1	−1.92±1.36	−0.58±0.12	−0.22±0.15	−0.18±0.3	−0.07±0.05
NM_019192	Selenoprotein P, plasma, 1	−1.86±0.14	−0.48±0.13	−0.12±0.13	0.23±0.23	0.16±0.48
M11842	Ornithine aminotransferase	−1.84±0.57	−1.04±0.23	−0.24±0.20	0.73±0.33	−0.27±0.64
AF205717	Transmembrane 4 superfamily member 4	−1.68±0.92	−0.66±0.07	−0.32±0.22	0.02±0.37	−0.68±0.37
NM_019286	Alcohol dehydrogenase 1	−1.67±0.42	−0.47±0.21	−0.16±0.19	0.21±0.18	−0.22±0.29
X05341	Acetyl-coenzyme A acyltransferase 2	−1.65±0.35	−0.24±0.25	−0.07±0.17	−0.12±0.16	−0.11±0.23
U25808	Kidney androgen regulated protein	−1.39±0.07	−1.51±0.61	−2.03±1.00	0.98±0.17	−0.80±0.13
Cluster D						
M32510	Hemoglobin alpha, adult chain 1	−0.64±0.43	−0.35±0.47	−1.25±0.40	−0.88±0.28	−0.44±0.98
AF005099	Neuronal pentraxin receptor	−0.56±0.48	−0.38±0.46	−1.19±0.49	−0.15±1.10	−0.41±0.87
M32509	Hemoglobin beta chain complex	−0.83±0.17	−0.57±0.24	−1.11±0.27	−0.75±0.11	−0.41±0.80
Cluster E						
U06274	UDP glycosyltransferase 2 family, polypeptide B4	−0.99±1.97	0.59±1.54	−1.33±2.05	0.62±1.17	1.12±0.46

The values shown are means of the log 2 ratios of (irreversible model/reversible model) samples ± s.d. Thus, a positive value indicates differential expression in the irreversible model, and a negative value indicates differential expression in the reversible model.
Cluster C contains 170 genes, but this table shows only the 14 genes whose expression level was three-fold or more different in the reversible model than in the irreversible model at one or more time points.

initiated kidney disease, and thus is regarded as the model that most closely mimics human chronic nephritis.

The microarray analysis of the irreversible model and reversible model identified 189 differentially expressed genes. Interestingly, the differential expression of the majority of these genes was found on day 4, and the mRNA expression of very few genes differed later. Thus, early alterations in gene expression may determine the irreversibility of the disease. This possibility was investigated by Ostendorf *et al.*[6] They found that early treatment prevented progression of the disease in irreversible anti-Thy-1 nephritis. When oligonucleotide aptamer antagonist against PDGF-B, which specifically inhibits PDGF activity, is administered on days 3 and 7 of the irreversible anti-Thy-1 nephritis model, the subsequent sclerotic lesions are less severe.

Clustering analysis of the differentially expressed genes was performed based on their temporal expression patterns to clarify the function, and the differentially expressed genes were classified into five clusters. The most interesting cluster was cluster A. The genes in cluster A were upregulated in the diseased kidney and were more strongly expressed in the irreversible model than in the reversible model. Cluster A contained the genes encoding collagen I $\alpha 1$ and laminin $\gamma 1$, which are profibrotic genes associated with the deposition of extracellular matrix. It also contained the genes encoding KIM-1, osteopontin, and thymosin $\beta 10$.

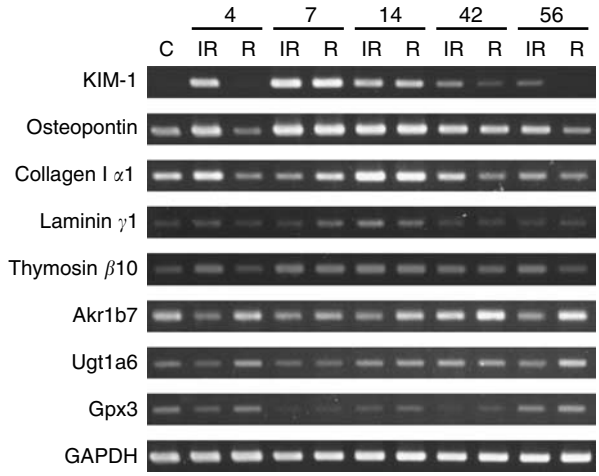

Figure 3 | Semiquantitative RT-PCR for the selected genes in the kidney in the reversible and irreversible models of anti-Thy-1 nephritis. mRNA was prepared from kidneys of the control rats (C), irreversible model rats (IR), and reversible model rats (R) at the times indicated and subjected to semiquantitative RT-PCR. Kidney injury molecule-1 (KIM-1), osteopontin, collagen I α1, laminin γ1, and thymosin β10 belong to cluster A. Aldo-keto reductase family 1, member B7 (Akr1b7), uridine diphosphate glycosyltransferase 1 family, polypeptide A6 (Ugt1a6), and glutathione peroxidase 3 (Gpx3) belong to cluster C.

KIM-1 is a type 1 membrane protein with extracellular immunoglobulin and mucin domains. KIM-1 is expressed at very low levels in the normal kidney, but its expression increases dramatically in the proximal tubule epithelial cells of the postischemic kidney.[7] We found that KIM-1 is upregulated in the anti-Thy-1 nephritis models, and more strongly expressed in the irreversible model. The increase in expression in the UUO model peaked at day 4, and it gradually decreased thereafter, suggesting that KIM-1 is associated with the initial insult rather than with progression of the disease. This is supported by the observation that KIM-1 is strongly expressed in acute renal failure, but weakly expressed in chronic renal disease.[8]

Osteopontin is a potent chemotactic molecule for macrophages, and upregulated expression by proximal tubular epithelial cells in association with monocyte/macrophage infiltrates has been described in a number of rodent models of renal injury and in human renal diseases.[9–11] Thymosin β10 is a small acidic peptide that binds to G-actin and inhibits actin polymerization. Overexpression of thymosin β10 has been detected in many neoplastic tissues, and thymosin β10 is known to inhibit angiogenesis and accelerate apoptosis.[12–14] Although expression of thymosin β10 has been reported to be upregulated in the developing kidney,[15,16] there have been no reports on involvement in kidney disease. In this study, we for the first time found that thymosin β10 is upregulated in the anti-Thy-1 nephritis models and the UUO model. The thymosin β10 was localized in the fibrotic interstitium. Double immunostaining with the macrophage marker ED-1 revealed that most of the cells that were positive for thymosin β10 were macrophages. Although there have been a few studies on thymosin β10 expression in monocytes/macrophages,[17–19] little is known about the function of thymosin β10 in macrophages.

Based on the overexpression of osteopontin and thymosin β10 in the irreversible Thy-1 model and the UUO model, we speculate that a possible mechanism for the common pathway of the progression of renal diseases involves macrophage infiltration and activation in the fibrotic interstitium. Although interstitial fibrosis of the irreversible model of anti-Thy-1 nephritis has not been investigated extensively, we observed significant infiltration of macrophages in the tubulointerstitium of the irreversible Thy-1 model (Figure 6e). In the UUO model, a large number of blood-derived macrophages accumulate in the tubulointerstitial space.[20] The infiltrating macrophages have been shown to play a pivotal role in the development of interstitial fibrosis in the UUO model. Lack of chemokines receptor CCR1 reduced recruitment of leukocytes and macrophages and suppressed renal fibrosis in the UUO model.[21] Interstitial macrophages are a common feature of most forms of progressive renal damage, including those not generally considered to be inflammatory, such as diabetic nephropathy.[22] At this time, we do not know the mechanism responsible for the greater upregulation of osteopontin and thymosin β10 in unilaterally nephrectomized rats.

Cluster C is the largest cluster, and is characterized by differential expression in the reversible model at day 4. Semiquantitative RT-PCR analysis of selected genes in cluster C revealed that the change in the ratio of expression levels at day 4 reflects decreased expression in the irreversible model. The majority of the genes, including the genes encoding transporters (aquaporin 1 and 4, anion exchange protein 1, and bumetanide-sensitive Na–K–2Cl cotransporter), kidney-specific androgen-regulated protein, megalin, Tamm-Horsfall protein, and carbonic anhydrase 2, are constitutively expressed in tubular cells, suggesting that anti-Thy-1 antibody induces early severer damage not only in glomerular cells but also in the tubular cells in the remaining kidney of nephrectomized rats than unnephrectomized rats. The damage may lead to decreased expression of genes that are constitutively expressed in tubular cells.

Unilateral nephrectomy itself may affect the remaining kidney. When the same microarray slide was used to compare gene expression in unilaterally nephrectomized rats not injected with mAb and control rats, no genes were found to be differentially expressed. Although we cannot detect differential expression, micropuncture studies have revealed that glomerular capillary hydraulic pressure and the glomerular transcapillary pressure difference increase significantly after nephrectomy.[23] A rise in glomerular capillary hydraulic pressure increases capillary wall tension, and the resulting stretching of the capillary wall stimulates endothelial expression of cell adhesion molecules,[24] and induces the production of vasoactive substances and cytokines, such as angiotensinogen and transforming growth factor-β, by injured or activated endothelium, which may exacerbate glomerular inflammation and lead to progressive glomerulosclerosis.

Table 3 | Genes whose expression in the kidney differed between the reversible model and the irreversible model of anti-Thy-1 nephritis at day 42

Gene accession	Name	log 2 ratio
Irreversible model > reversible model		
AF091577	Olfactory receptor gene Olr1370	2.02 ± 0.18
NM_012881	Osteopontin	1.98 ± 0.23
AF198087	Adrenal secretory serine protease precursor	1.93 ± 0.04
NM_012868	Natriuretic peptide receptor 3	1.80 ± 0.13
AF016178	Putative pheromone receptor (Go-VN1)	1.61 ± 0.05
X89698	Olfactory receptor gene Olr737	1.41 ± 0.59
AF035963	Kidney injury molecule 1	1.34 ± 0.21
U56822	Killer cell lectin-like receptor subfamily A, member 22	1.25 ± 0.26
U87224	Contactin associated protein 1	0.95 ± 0.31
U48828	Retroviral-like ovarian specific transcript 30-1	0.93 ± 0.48
NM_017217	Solute carrier family 7, member 3	0.84 ± 0.22
M16758	Small cytoplasmic RNA (alpha-1-RNA)	0.83 ± 0.18
M58404	Thymosin, beta 10	0.82 ± 0.19
M64387	Olr1493	0.79 ± 0.27
NM_012862	Matrix Gla protein	0.75 ± 0.43
M11842	Ornithine aminotransferase	0.73 ± 0.33
NM_012679	Testosterone-repressed prostate message 2	0.71 ± 0.04
M35601	Fibrinogen, alpha polypeptide	0.69 ± 0.26
X94551	Laminin, gamma 1	0.67 ± 0.37
NM_017184	Troponin I, skeletal, slow 1	0.66 ± 0.29
NM_013043	Transforming growth factor beta stimulated clone 22	0.65 ± 0.22
AF097887	Ras homolog gene family, member V	0.60 ± 0.35
D86742	Cadherin 4	0.60 ± 0.24
M34043	Thymosin, beta 4	0.58 ± 0.26
AF010437	MARRLC2A	0.58 ± 0.34
Irreversible model < reversible model		
M33936	Cytochrome P450, family 4, subfamily a, polypeptide 14	−1.21 ± 0.11
NM_017260	Arachidonate 5-lipoxygenase activating protein	−1.01 ± 0.17
M32510	Hemoglobin alpha, adult chain 1	−0.88 ± 0.28
NM_012588	Insulin-like growth factor binding protein 3	−0.86 ± 0.12
M32509	Hemoglobin beta chain complex	−0.75 ± 0.11
U29881	Solute carrier family 5 (sodium/glucose cotransporter), member 2	−0.71 ± 0.06
M11563	Nerve growth factor, gamma	−0.68 ± 0.33
NM_017235	Hydroxysteroid (17-beta) dehydrogenase 7	−0.66 ± 0.27
NM_012677	Tonin	−0.62 ± 0.25
AJ238392	Similar to sulfotransferase K1	−0.61 ± 0.23
X63854	Ransporter 2, ATP-binding cassette, sub-family B	−0.60 ± 0.19
AF168362	Hspb associated protein 1	−0.58 ± 0.33
NM_017013	Glutathione transferase YA subunit	−0.57 ± 0.17
J00719	Cytochrome P450, 2b19	−0.57 ± 0.19

The values shown are means of the log2 ratios of (irreversible model/reversible model) samples ± s.d. Thus, a positive value indicates differential expression in the irreversible model, and a negative value indicates differential expression in the reversible model.

A possible criticism of the effect of nephrectomy is the difference in the amount of kidney binding mAb 1-22-3 in the nephrectomized and intact rats. However, our previous quantitative study with various doses of mAb 1-22-3 showed no significant difference in infiltrating cells or severity of mesangial alterations between rats injected with 0.5 and 10 mg.[3,25] Even when the rats were injected with a single dose of mAb 1-22-3 and subjected to unilateral nephrectomy, they exhibited a progressive course.[26] These observations indicate that the difference in the amount of kidney binding antibody between the sham-operated group and unilaterally nephrectomized group had little effect with regard to the different outcomes of the disease. We therefore speculate that nephrectomy may cause 'cell priming' that induces no more than very subtle, barely detectable changes in the cells, and that injection of mAb 1-22-3 into the primed cells injures them beyond the threshold of no return.

In conclusion, the microarray analysis in the irreversible model and reversible model of anti-Thy-1 nephritis identified 189 differentially expressed genes, and they were classified into five clusters. Genes that are constitutively expressed in tubular cells were downregulated in the irreversible model at day 4, suggesting that mAb 1-22-3 causes more severe injury to tubular cells as well as glomerular cells in nephrectomized rats than in unnephrectomized rats. Genes belonging to cluster A were more strongly expressed in the irreversible model, and overexpression of osteopontin and thymosin $\beta 10$ persisted in the irreversible anti-Thy-1 nephritis model and in the UUO model. The overexpression of osteopontin, a potent macrophage chemoattractant, and of thymosin $\beta 10$ suggests that macrophage infiltration and activation play a

Table 4 | Genes whose expression in the kidney differed between the reversible model and the irreversible model of anti-Thy-1 nephritis at day 56

Gene accession	Name	log 2 ratio
Irreversible model > reversible model		
U06274	UDP glycosyltransferase 2 family, polypeptide B4	1.12 ± 0.46
AF091577	Olfactory receptor gene Olr1370	1.05 ± 0.19
NM_012881	Osteopontin	1.03 ± 0.07
AF198087	Adrenal secretory serine protease precursor	0.97 ± 0.22
AF035963	Kidney injury molecule 1	0.95 ± 0.36
NM_012868	Natriuretic peptide receptor 3	0.95 ± 0.27
AF016178	Putative pheromone receptor (Go-VN1)	0.92 ± 0.21
X89698	Olfactory receptor gene Olr737	0.87 ± 0.15
NM_012862	Matrix Gla protein	0.77 ± 0.13
U56822	Killer cell lectin-like receptor subfamily A, member 22	0.77 ± 0.36
M58404	Thymosin, beta 10	0.76 ± 0.22
M64387	Olr1493	0.75 ± 0.20
J00705	Apolipoprotein E	0.75 ± 0.35
M12199	Collagen, type I, alpha 1	0.73 ± 0.28
M35601	Fibrinogen, alpha polypeptide	0.68 ± 0.21
NM_013043	Transforming growth factor beta stimulated clone 22	0.66 ± 0.13
U69487	ATP-binding cassette, sub-family B (MDR/TAP), member 11	0.66 ± 0.29
NM_017184	Troponin I, skeletal, slow 1	0.65 ± 0.28
U42719	Complement component 4, gene 2	0.64 ± 0.38
NM_012679	Testosterone-repressed prostate message 2	0.64 ± 0.34
NM_013098	Glucose-6-phosphatase, catalytic	0.60 ± 0.18
Irreversible model < reversible model		
S62516	SA rat hypertension-associated homolog	−1.38 ± 0.39
U48828	Retroviral-like ovarian specific transcript 30-1	−0.92 ± 0.40
AF053988	Tissue-type vomeronasal neurons putative pheromone receptor V2R1-1	−0.91 ± 0.52
D10693	Histamine N-methyltransferase	−0.75 ± 0.33
M55250	Glycine receptor, alpha 3 subunit	−0.74 ± 0.35
NM_012909	Aquaporin 2	−0.74 ± 0.25
S81497	Lipase A, lysosomal acid	−0.69 ± 0.34
NM_012817	Insulin-like growth factor binding protein 5	−0.69 ± 0.41
AF205717	Transmembrane 4 superfamily member 4	−0.68 ± 0.37
AF060173	SV2 related protein	−0.67 ± 0.26
U24070	Unc-13 homolog A	−0.62 ± 0.35
NM_019282	Gremlin 1 homolog, cysteine knot superfamily	−0.61 ± 0.23
AJ295749	Xylosyltransferase II	−0.60 ± 0.28
M92042	N-deacetylase/N-sulfotransferase (heparan glucosaminyl) 1	−0.60 ± 0.34
NM_017136	Squalene epoxidase	−0.59 ± 0.27
AF264005	Fucosyltransferase 2 (secretor status included)	−0.59 ± 0.22

The values shown are means of the log 2 ratios of (irreversible model/reversible model) samples ± s.d. Thus, a positive value indicates differential expression in the irreversible model, and a negative value indicates differential expression in the reversible model.

crucial role in progression of the renal diseases. The mechanism of overexpression of osteopontin and thymosin β10 in the irreversible model remains to be elucidated. Further investigation of thymosin β10 may illuminate the nature of progression of renal diseases.

MATERIALS AND METHODS

Animal models

Female Wistar rats, 6 weeks old, were used. The irreversible model of anti-Thy-1 nephritis was induced as previously described.[27,28] Briefly, rats were unilaterally nephrectomized and 1 week later intravenously injected with 0.5 mg of mAb 1-22-3. The reversible model of anti-Thy-1 nephritis was induced by injecting sham-operated rats with the same dose of antibody. Rats were killed on days 4, 7, 14, 42, and 56 after the injection (at least four rats each time). As a control, four rats were unilaterally nephrectomized, not injected with antibody, and were killed on day 56.

The UUO model was produced by ligating the left ureter at two sites and transecting it between the ligations.[9] Rats were killed on days 1, 3, 7, 14, and 21 after surgery, and the contralateral kidneys were used as intraindividual controls.

Rats were killed under anesthesia, and cross-sections of kidneys were fixed in 10% neutral buffered formalin for paraffin sections and in 4% paraformaldehyde for cryosections, and the remaining portions of the kidney were snap-frozen in liquid nitrogen for RNA isolation. Sections for histologic examination were stained with periodic acid–Schiff reagent.

Urinary protein excretion was measured by the Pyrogallol Red method before the antibody injection, and 4, 7, 14, 21, 24, 42, 49, and 56 days after the antibody injection. The rats were given free access to water in individual metabolic cages for collection of 24-h urine specimens. All procedures used in the animal experiments complied with the standards described in the Guidelines for the Care and Use of Laboratory Animals of Keio University School of Medicine.

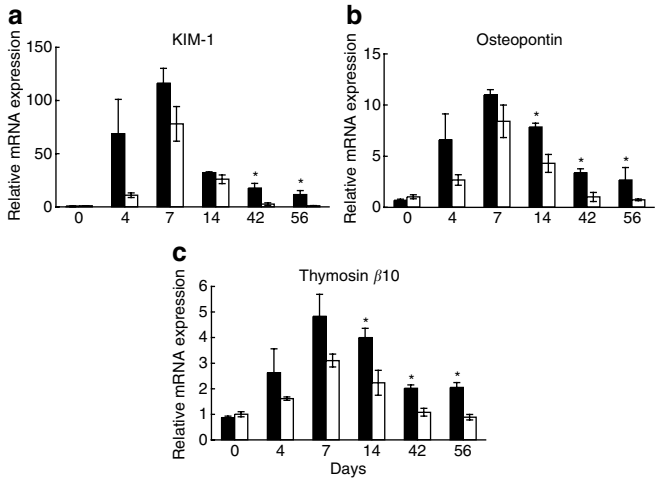

Figure 4 | Real-time PCR for the selected genes in the kidney in the reversible and irreversible models of anti-Thy-1 nephritis. mRNA was prepared from the kidneys of the irreversible and reversible model rats at times indicated and subjected to real-time (**a**) PCR for KIM-1, (**b**) osteopontin, and (**c**) thymosin β10. The black and white bars at each time point represent expression in the irreversible and the reversible nephritis kidney, respectively. Data were normalized for the amount of 18S ribosomal RNA in each sample and are expressed relative to the value measured in the control sample. Mean values $\pm$ s.e.m. are shown. *$P<0.05$ compared to the reversible model at the same time point.

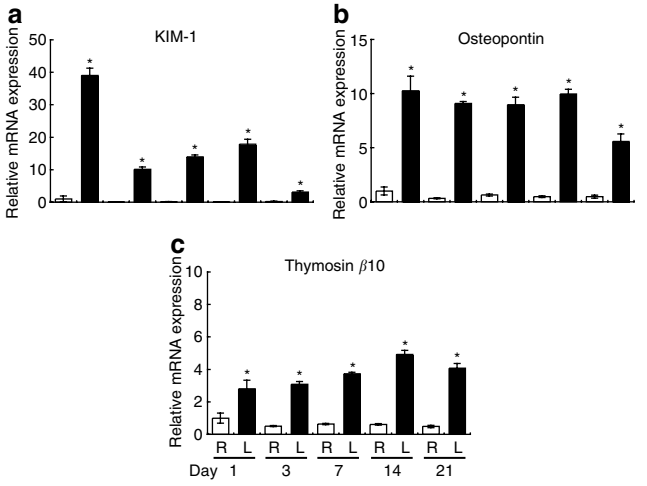

Figure 5 | Real-time PCR for the selected genes in the unilateral ureteral obstruction model. mRNA was prepared from unobstructed right kidneys (R, white bar) and obstructed left kidney (L, black bar) at the times indicated, and subjected to real-time PCR for (**a**) KIM-1, (**b**) osteopontin, and (**c**) thymosin β10. Data were normalized for the amount of 18S ribosomal RNA in each sample and expressed relative to the value measured in the kidney on the side at day 1. Mean values $\pm$ s.e.m. are shown. *$P<0.05$ compared to the value in the contralateral kidneys.

Microarray experiments

cDNA probes were synthesized from 2.0 μg of poly(A)$^+$ RNA by a two-step procedure using the CyScribe Post-Labeling Kit (Amersham Biosciences Corp., Piscataway, NJ, USA). In the first step, amino allyl-dUTP was incorporated into first-strand cDNA during reverse transcription. In the second step, the amino allyl-modified cDNA was chemically labeled with CyDye™ NHS-esters (either Cy3

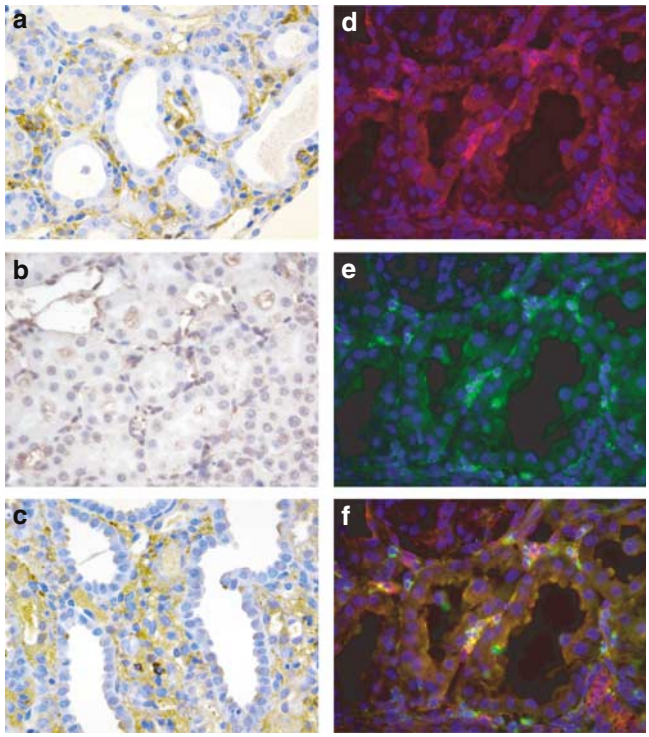

Figure 6 | Imunohistochemical localization of thymosin β10. Expression of thymosin β10 was immunolocalized in the kidney in the (**a**) irreversible anti-Thy-1 nephritis model at day 14, (**b**) in the reversible anti-Thy-1 nephritis model at day 14, and (**c**) in the unilateral ureteral obstruction model at day 7. Brown represents immunopositivity; nuclei are stained blue. (**d**–**f**) Double immunostaining of the kidney in the irreversible anti-Thy-1 nephritis model at day 14 with anti-thymosin β10 antibody and the macrophage marker ED-1. Nuclei were visualized by blue 4,6-diamidino-2-phenylindole staining. (**d**) Immunoreactivity for thymosin β10 was visualized with red. (**e**) Immunoreactivity for ED-1 was visualized with green. (**f**) Merged image. (Original magnification $\times$ 400).

or Cy5 signal). The Cy3- or Cy5-labeled cDNA probes were then combined and diluted in 30 μl of ArrayHyb™ Low Temp Hybridization Buffer (Sigma, St Louis, MO, USA).

Oligonucleotide microarrays with approximately 4854 rat genes (DNA chip consortium, Sigma Genosys Japan, Hokkaido, Japan) were used. Microarray slides were prehybridized in 5 $\times$ SSC, 0.1% SDS, and 1% BSA at 42°C for 1 h. Labeled cDNA probes were hybridized with the microarray slides by overnight incubation at 42°C. The slides were washed with 1 $\times$ SSC and 0.03% SDS at 42°C for 4 min, then with 0.2 $\times$ SSC at room temperature for 4 min, and finally with 0.05 $\times$ SSC at room temperature for 4 min. Hybridization images were scanned with a GenePix 4000A scanner (Axon Instrument Inc., Foster City, CA, USA), and the fluorescence intensity of Cy3 and Cy5 was quantitated with GenePix Pro 3.0 software (Axon Instrument Inc.). To avoid the effect of putative artificial signals caused by nonspecific dye–cDNA interactions, each hybridization was performed twice, where the second experiment was performed with a reversed Cy-dye assignment (the so-called 'dye flip'). At least four hybridizations were performed at each time point.

The ratio of the Cy3 to Cy5 signal intensity (Cy3/Cy5) was $\log_2$-transformed, and each $\log_2$(Cy3/Cy5) value was normalized by subtracting the average of the $\log_2$(Cy3/Cy5) values for the glyceraldehyde 3-phosphate dehydrogenase genes. Genes with median $\log_2$ values for the ratios $\geqslant 1$ or $\leqslant -1$ were considered

upregulated (two-fold or more) or downregulated (two-fold or more), respectively. Average-linkage hierarchical clustering analysis was applied to the 189 differentially expressed genes with clustering software Cluster 3.0 (http://bonsai.ims.u-tokyo.ac.jp/~mdehoon/software/cluster/) and visualized by Java TreeView 1.0.4 (http://genetics.stanford.edu/~alok/TreeView/).

Semiquantitative RT-PCR and real-time PCR

For semiquantitative analysis, the number of amplification cycle of PCR was determined in the exponential phase. Glyceraldehyde dehydrogenase mRNA levels were used to standardize the mRNA levels of the target genes.

Real-time PCR was performed as described previously.[29] The PCR primers and TaqMan probes were designed using Primer Express software 1.5 (Applied Biosystems, Foster City, CA, USA). The RNA sample (50 μg) was exposed to DNase to remove the DNA, and then amplified with TaqMan Gold PCR Reagents (Applied Biosystems). The PCR reactions were monitored in real time with the ABI PRISM 7700 Sequence Detector (Applied Biosystems). All data were normalized by using 18S ribosomal RNA as an endogenous control.

Immunohistochemical study

Paraffin sections were deparaffinized and hydrated, and antigen was retrieved by boiling the tissue for 10 min in 10 mM citric acid, pH 6.0. After washes, the slides were hybridized with anti-thymosin β10 antibody (Biodesign International, Saco, ME, USA) at 4°C overnight. The anti-thymosin β10 antibody was raised against the human thymosin β10 peptide (aa 1–12) and does not crossreact with other subtypes of β-thymosin. Antigen-bound primary antibody was detected with the DAKO LSAB2 Kit (Dako, Carpinteria, CA, USA). The chromogen substrate was diaminobenzidine, and the sections were counterstained with hematoxylin.

For double immunostaining, cryosections were incubated with anti-thymosin β10 antibody and monoclonal antibody ED-1 (Chemicon International Inc., Temucula, CA, USA). Alexa Fluor 594-conjugated anti-rabbit IgG and Alexa Fluor 488-conjugated anti-mouse IgG (Invitrogen Corp., Carlsbad, CA, USA) were used as secondary antibodies. The nuclei were stained with 4,6-diamidino-2-phenylindole.

Statistical analysis

Statistical significance was evaluated by Student's *t*-test or one-way analysis of variance with a Fisher's *post hoc* test, as appropriate. Statistical significance was defined as $P<0.05$. All values are expressed as means $\pm$ s.e.m.

ACKNOWLEDGMENTS

This work was supported, in part, by grants from the Ministry of Education, Science and Culture of Japan, a Keio University Grant-in-Aid for Encouragement of Young Medical Scientists, and a National Grant-in-Aid for the Establishment of High-Tech Research Center in a Private University. The full data set can be seen at the GEO site http://www.ncbi.nlm.nih.gov/projects/geo/ (accession nos. GSM72509–72513).

REFERENCES

1. Yamamoto T, Yamamoto K, Kawasaki K *et al.* Immunoelectron microscopic demonstration of Thy-1 antigen on the surfaces of mesangial cells in the rat glomerulus. *Nephron* 1986; **43**: 293–298.
2. Kawachi H, Orikasa M, Matsui K *et al.* Epitope-specific induction of mesangial lesions with proteinuria by a MoAb against mesangial cell surface antigen. *Clin Exp Immunol* 1992; **88**: 399–404.
3. Kawachi H, Oite T, Shimizu F. Quantitative study of mesangial injury with proteinuria induced by monoclonal antibody 1-22-3. *Clin Exp Immunol* 1993; **92**: 342–346.
4. Cheng QL, Orikasa M, Morioka T *et al.* Progressive renal lesions induced by administration of monoclonal antibody 1-22-3 to unilaterally nephrectomized rats. *Clin Exp Immunol* 1995; **102**: 181–185.
5. Shimizu F, Kawachi H, Orikasa M. Role of mesangial cell damage in progressive renal disease. *Kidney Blood Press Res* 1999; **22**: 5–12.
6. Ostendorf T, Kunter U, Grone HJ *et al.* Specific antagonism of PDGF prevents renal scarring in experimental glomerulonephritis. *J Am Soc Nephrol* 2001; **12**: 909–918.
7. Ichimura T, Bonventre JV, Bailly V *et al.* Kidney injury molecule-1 (KIM-1), a putative epithelial cell adhesion molecule containing a novel immunoglobulin domain, is up-regulated in renal cells after injury. *J Biol Chem* 1998; **273**: 4135–4142.
8. Han WK, Bailly V, Abichandani R *et al.* Kidney Injury Molecule-1 (KIM-1): a novel biomarker for human renal proximal tubule injury. *Kidney Int* 2002; **62**: 237–244.
9. Kaneto H, Morrissey J, McCracken R *et al.* Osteopontin expression in the kidney during unilateral ureteral obstruction. *Miner Electrolyte Metab* 1998; **24**: 227–237.
10. Xie Y, Sakatsume M, Nishi S *et al.* Expression, roles, receptors, and regulation of osteopontin in the kidney. *Kidney Int* 2001; **60**: 1645–1657.
11. Pichler R, Giachelli CM, Lombardi D *et al.* Tubulointerstitial disease in glomerulonephritis. Potential role of osteopontin (uropontin). *Am J Pathol* 1994; **144**: 915–926.
12. Huff T, Muller CS, Otto AM *et al.* beta-Thymosins, small acidic peptides with multiple functions. *Int J Biochem Cell Biol* 2001; **33**: 205–220.
13. Lee SH, Son MJ, Oh SH *et al.* Thymosin \{beta\}(10) inhibits angiogenesis and tumor growth by interfering with Ras function. *Cancer Res* 2005; **65**: 137–148.
14. Hall AK. Thymosin beta-10 accelerates apoptosis. *Cell Mol Biol Res* 1995; **41**: 167–180.
15. Hall AK. Differential expression of thymosin genes in human tumors and in the developing human kidney. *Int J Cancer* 1991; **48**: 672–677.
16. Rosenblum ND, Yager TD. Changing patterns of gene expression in developing mouse kidney, as probed by differential mRNA display combined with cDNA library screening. *Kidney Int* 1997; **51**: 920–925.
17. Lapteva N, Ando Y, Nieda M *et al.* Profiling of genes expressed in human monocytes and monocyte-derived dendritic cells using cDNA expression array. *Br J Haematol* 2001; **114**: 191–197.
18. Gutierrez-Pabello JA, McMurray DN, Adams LG. Upregulation of thymosin beta-10 by *Mycobacterium bovis* infection of bovine macrophages is associated with apoptosis. *Infect Immun* 2002; **70**: 2121–2127.
19. Yu FX, Lin SC, Morrison-Bogorad M *et al.* Effects of thymosin beta 4 and thymosin beta 10 on actin structures in living cells. *Cell Motil Cytoskeleton* 1994; **27**: 13–25.
20. Schreiner GF, Harris KP, Purkerson ML *et al.* Immunological aspects of acute ureteral obstruction: immune cell infiltrate in the kidney. *Kidney Int* 1988; **34**: 487–493.
21. Eis V, Luckow B, Vielhauer V *et al.* Chemokine receptor CCR1 but not CCR5 mediates leukocyte recruitment and subsequent renal fibrosis after unilateral ureteral obstruction. *J Am Soc Nephrol* 2004; **15**: 337–347.
22. Kluth DC, Erwig LP, Rees AJ. Multiple facets of macrophages in renal injury. *Kidney Int* 2004; **66**: 542–557.
23. Miller PL, Rennke HG, Meyer TW. Glomerular hypertrophy accelerates hypertensive glomerular injury in rats. *Am J Physiol* 1991; **261**: F459–F465.
24. Nagel T, Resnick N, Atkinson WJ *et al.* Shear stress selectively upregulates intercellular adhesion molecule-1 expression in cultured human vascular endothelial cells. *J Clin Invest* 1994; **94**: 885–891.
25. Sakai N, Iseki K, Suzuki S *et al.* Uninephrectomy induces progressive glomerulosclerosis and apoptosis in anti-Thy1 glomerulonephritis. *Pathol Int* 2005; **55**: 19–26.
26. Wada Y, Morioka T, Oyanagi-Tanaka Y *et al.* Impairment of vascular regeneration precedes progressive glomerulosclerosis in anti-Thy 1 glomerulonephritis. *Kidney Int* 2002; **61**: 432–443.
27. Ito Y, Kawachi H, Morioka Y *et al.* Fractalkine expression and the recruitment of CX3CR1+ cells in the prolonged mesangial proliferative glomerulonephritis. *Kidney Int* 2002; **61**: 2044–2057.
28. Asai M, Monkawa T, Marumo T *et al.* Spironolactone in combination with cilazapril ameliorates proteinuria and renal interstitial fibrosis in rats with anti-Thy-1 irreversible nephritis. *Hypertens Res* 2004; **27**: 971–978.
29. Yoshino J, Monkawa T, Tsuji M *et al.* Leukemia inhibitory factor is involved in tubular regeneration after experimental acute renal failure. *J Am Soc Nephrol* 2003; **14**: 3090–3101.